

# California Institute of Technology

## Graduate Aeronautics Laboratory



### **Tunable Highly-Nonlinear Acoustic Waves**

and their coupling with

### **Linear Elastic Media**

Keck Institute for Space Studies Graduate Student Fellowship Final Report

By  
**Devvrath Khatri**  
Advisor: Dr. Chiara Daraio

September 2010

## Acknowledgement

I would like to convey my utmost gratitude to my advisor Dr. Chiara Daraio for her advice, guidance and encouragement throughout the research.

Secondly I owe many thanks to Dr. Jinkyu Yang, Dr. Alessandro Spadoni, Dr. Duc Ngo, Dr. Abha Misra for their useful advice and support in numerics and experiments to carry out the research work. I am also thankful to Petros Arakelian for his suggestions and help in building experimental setup. I wish to express my thanks to Chinthaka Mallikarachchi and Xiaowei Deng at Caltech, USA for suggestion on finite element simulations.

Further, I would like to thank all of the Highly Nonlinear Group at Graduate Aeronautical Laboratories , Caltech for their constructive suggestions and helpful discussions.

Last but not least I am grateful to my parents for their understanding and support.

## Acknowledgement to KISS

W.M. Keck Institute for Space Studies,  
Graduate Student Fellowship,  
California Institute of Technology,  
Pasadena, CA, 91125

Members of Keck Institute for Space Studies,

I will like to express my sincere gratitude to W.M. Keck Institute for Space Studies (KISS) for your Graduate Student Fellowship. I am grateful to be considered as the recipient of your scholarship.

I am a final year Ph.D. student in Aeronautics at California Institute of Technology (Caltech) and plan to graduate in Spring of 2011. After graduation, I would like to pursue my career as a research scientist/engineer. The KISS Graduate Student Fellowship award has helped me in covering my financial expenses and allowed me to focus my time on research and learning. This fellowship enabled me to pay the expenses of using high performance computing cluster for my research purpose and also allowed me to attend the summer school in Italy on “Wave Propagation in Linear and Nonlinear Periodic Media: Analysis and Applications”.

KISS Graduate Student Fellowship was crucial in allowing me to have the support and freedom to explore the research topics that I am interested in. The financial support of the Keck Institute For Space Studies is greatly appreciated and it is their generosity that made this research possible.

Thank You,

Sincerely,

Devvrath Khatri

## Abstract

This project aims at introducing and testing a new method of Non-Destructive Evaluation (NDE) and Structural Health Monitoring (SHM) for materials and engineering systems, based on the use of Highly Nonlinear Acoustic Waves (HNAWs). At a fundamental level the project aims at understanding the interface behavior between linear and highly nonlinear media. The effects of interface dynamics on the temporary localization of incident waves and their decomposition into reflected waves are investigated.

We implemented a finite element model for HNAWs formation and propagation in granular chain using commercially available software Abaqus. We validated our finite element model with the theoretical work of static loading between two beads using Hertz's law and for dynamic impact loading for the formation and propagation of solitary wave in the chain of beads using Nesterenko's theory. We also compared our results with discrete particle model and corroborate the results with experiments.

To use nonlinear actuator system for NDE/SHM applications purpose, we studied the losses in the energy transmission as wave propagate in chain of spherical beads. We proposed a quantitatively-accurate extension of the Hertzian model encompassing realistic material dissipative effects in a one-dimensional chain of granular materials. Using an optimization scheme, we computed the relevant exponents and prefactors of the dissipative terms in the equations of motion. Using linear Rayleigh damping we modeled the dissipation effects in the finite element simulations. We used the root mean square deviation method to obtained the optimized mass proportional factor of damping. The experimental results are found to be in good agreement with proposed model in terms of wave amplitude and wave shape.

To understand the coupling of nonlinear media with adjacent linear elastic media, we studied experimentally and numerically the effects of solitary waves interacting with different single- and multi-layered media. We performed the theoretical analysis of the coupling based on the long-wavelength approximation in a one-dimensional chain of beads. The numerical predictions based on discrete particle model and experimental results are in good agreement with the theoretical analysis. In our study, we found a correlation between the properties of reflected waves from the interface and the elastic modulus of adjacent linear elastic media. For elastic modulus value below the critical limit, we monitored the generation of secondary reflected solitary waves at the interface and found the dependence of them on the ratio of elastic modulus of adjacent media and of the spherical particles.

In order to understand the coupling of nonlinear actuator system with the composite media for NDE/SHM purpose, we further extended our study for the interaction of highly nonlinear acoustic waves with double layered media. The results shows a correlation between the properties of primary reflected waves with the inertia of the top layer and the dependence of properties of secondary reflected solitary waves on the bottom layer. The results were found in good agreement with the experimental finding.

The work done as part of this research enhances our understanding on the basic physics and tunability of nonlinear media, and further establishes a theoretical and numerical foundation in the applications of NDE/SHM in various areas.

# Table of Contents

|  |           |
|--|-----------|
| Acknowledgement  | i         |
| Acknowledgement to KISS  | ii        |
| Abstract   | iii       |
| Table of Contents  | iv        |
| List of Figures  | v         |
| <b>1 Introduction</b>  | <b>1</b>  |
| 1.1 Introduction to Granular Media . . . . .   | 1         |
| 1.2 Scope and Aim . . . . .  | 2         |
| 1.3 Outline of the Report . . . . .  | 2         |
| <b>2 Highly-Nonlinear acoustic waves in one-dimensional chain of spherical particles</b> | <b>3</b>  |
| 2.1 Theoretical Background . . . . .   | 3         |
| 2.2 Experimental Setup . . . . .   | 4         |
| 2.3 Simulation . . . . .   | 5         |
| 2.3.1 Discrete Particle Model . . . . .  | 5         |
| 2.3.2 Finite Element Model . . . . .   | 5         |
| <b>3 Dissipation in one-dimensional chain of spherical particles</b>                     | <b>8</b>  |
| 3.1 Experimental setup . . . . .   | 8         |
| 3.2 Simulation . . . . .   | 8         |
| 3.2.1 Discrete Empirical Model . . . . .   | 8         |
| 3.2.2 Finite Element Model . . . . .   | 9         |
| 3.3 Results . . . . .  | 9         |
| <b>4 Coupling of Nonlinear Media with Linear Media</b>                                   | <b>10</b> |
| 4.1 Interaction of highly nonlinear waves with a uniform medium . . . . .                | 10        |
| 4.1.1 Effects of the linear medium stiffness . . . . .                                   | 10        |
| 4.1.2 Effects of the linear medium geometry . . . . .                                    | 11        |
| 4.2 Interaction of highly nonlinear waves with a composite medium . . . . .              | 12        |
| 4.2.1 Effects of variable thickness of the upper layer of composite medium . . . . .     | 12        |
| 4.2.2 Effects of variable thickness of the lower layer of composite medium . . . . .     | 12        |
| <b>5 Conclusions and Future Work</b>   | <b>14</b> |
| 5.1 Conclusions . . . . .  | 14        |
| 5.2 Future Work . . . . .  | 14        |
| <b>Bibliography</b>  | <b>14</b> |

# List of Figures

|     |   |    |
|-----|---|----|
| 1.1 | Schematic diagram of nonlinear granular chain as an automated impact actuator inside a satellite. The reflected waves from the interface, buried defect/impurity and boundaries will be used to monitor the structure. . . . .  | 1  |
| 2.1 | Schematic diagram of the experimental setup consisting of spherical bead particles in granular chain. Four steel rods are used as guided rail to support the beads in the chain. An identical bead is used as striker to generate single pulse of wave. Schematic shows the sensor-particle connected with computer to collect the signal data of wave propagation. . . . .   | 5  |
| 2.2 | Quasi-Static Validation: (a) finite element model consisting of two spherical beads in Hertzian contact. The beads are given small displacement boundary condition and corresponding contact force is calculated from simulations. (b) the logarithmic fitting of the obtained contact force and applied displacement on the bead. The Y-axis and X-axis shows the contact force and $\delta$ in logarithmic scale respectively. The dot values are numerically obtained contact force for the corresponding displacement, the solid line is the linear fit (c) Comparison of power law obtained from simulations (solid curve) with the Hertz's theory (Eq 2.1, dashed curve) . . . . .  | 6  |
| 2.3 | (a) Finite element model showing the one-dimensional chain of spherical beads in contact with each other Force versus time plot for the solitary wave propagation in chain composing of 20 stainless steel beads (b) Experiments, (c) Discrete Hertz Law, (d) Abaqus simulation. The curves represent the wave propagation in particle number 10 (blue) and 15 (red) respectively from the top of the chain for striker velocity $0.626m/s$ . (e) Force-Velocity Scaling - The solid curve represents the theoretical value using Eq 2.6, the square marker represents the discrete particle model values and the dot marker represents the finite element value for Dependence of the solitary wave speed on the magnitude of the contact dynamic force. . . . . | 7  |
| 3.1 | a) Decay of solitary wave in chain of 70 stainless steel particles for striker velocity $= 1.77m/s$ . The sensor-particles are placed at 9, 16, 24, 31, 40, 50, 56, and 63 bead number and the solid curves (blue) corresponds to force value observe by them. The circle with solid curve (red), the triangle with solid curve (magenta) and the square with dashed curve (red) represents the maximum value of experimental, discrete particle and finite element model respectively. b) and c) . . . . .   | 9  |
| 4.1 | Finite element model for coupling of 1D chain of nonlinear media composed of 20 spherical beads particle with adjacent linear elastic media (a) a uniform linear medium and (b) a composite linear medium. The bottom of the linear media is under fixed boundary conditions. . . . .   | 10 |
| 4.2 | (a) Numerical results showing the surface plots of incident and reflected solitary waves in granular chain as a function of elastic modulus of the uniform linear media adjacent to the chain of spheres. The Y-axis reports a set of different values of elastic moduli of the linear media adjacent to the chain of spheres. As the stiffness of the contact is decreased, the TOF of the reflected wave increases. (b) Amplitude Reflection ratio of the amplitude of the PSW over that of the incident solitary wave. (c) Amplitude Reflection ratio of the amplitude of the SSW over the amplitude of the incident solitary wave. The reflection ratio becomes smaller as the elastic modulus increases. . . . .   | 11 |
| 4.3 | (a) Numerical results showing the surface plots of incident and reflected solitary waves in granular chain as a function of height of the uniform linear media adjacent to the chain of spheres. The Y-axis reports a set of different values of height of the linear media adjacent to the chain of spheres. The first band visible on the left represents the incoming solitary waves, while the band on the right shows the reflected solitary waves (PSWs). No secondary solitary wave is observed. (b) Amplitude Reflection ratio of the amplitude of the PSW over that of the incident solitary wave. Numerical results show a minute drop around the characteristic length of the linear medium. . . . .   | 11 |

|     |  |    |
|-----|--|----|
| 4.4 | Comparison of experimental, theoretical, and numerical results for the time of arrival time on the instrumented particle (TOF) and amplitude ratio of the primary and secondary reflected solitary waves in the chain of spheres, as a function of the upper layer thickness ( $L_u$ ) in the composite media. (a) TOF for the PSWs. The arrival time is within 0.43- to 0.47-ms range. (b) Amplitude ratio for the PSWs. The amplitude reflection ratio increases as $L_u$ grows. (c) Time of flight for the SSWs. Compared to that of the PSWs, the progression is in opposite direction with improved responsiveness. (d) Amplitude ratio of the SSWs. On the contrary to the PSW reflection in (b), larger $L_u$ yields the smaller SSW reflection in compensation for the increased PSW reflection. For the upper layer taller than 22 mm, the magnitude of the reflection ratio drops below 10 . . . . . | 12 |
| 4.5 | (a) Numerical results showing the surface plots of incident and reflected solitary waves in granular chain as a function of lower layer dimension of the composite linear media. The formation of the primary reflected solitary wave is insensitive to the lower layer thickness, showing the constant amplitude and arrival time for all lower layer thicknesses tested. However, the secondary solitary waves reveal significant delay in their formation as the dimension of the lower layer increases. (b) Amplitude reflection ratios of the PSWs. (c) Time of flight of the SSWs. as a function of lower medium height ( $L_d$ ). . . . .   | 13 |

# Chapter 1

## Introduction

### 1.1 Introduction to Granular Media

Acoustic waves are commonly used for monitoring engineering systems for identifying structural geometry, flaw and acoustic behavior of structures. In the last few decades several stress wave based inspection/monitoring techniques have been developed for damage detection and material characterization in metallic and composite structures [Shull, 2002]. Such detailed information on the nature of the damage comes at the cost of extended time of interrogation, heavy data processing and require significant external power supply. Thus, there is a widespread need for new NDE/SHM techniques, which can provide alternative solutions to long standing problems of actuation and signal generation, improve accuracy and detection resolution and provide novel solution for signal processing.

For this research we use granular systems to generate highly nonlinear acoustic waves as novel information carriers to interrogate structures, as an alternative to classical instrumented hammers used in impact testing (Fig 1.1). By granular material, we refer to the aggregate of discrete macroscopic particles. The size of the granular particle is on a comparable scale to size of total system and usually large enough such that they are not subject to thermal motion fluctuations. This granular materials interact with each other through dual nonlinearity, where in compression they follow a complete nonlinear behavior without any linear component and on the other side they have zero tensile force.

When this granular material are assembled in a linear or network shaped arrangement, the dual nonlinearity of the system and the heterogeneity of the scales places them in a special class of highly nonlinear behavior. In the highly nonlinear regime, the traditional linear and weakly nonlinear continuum approach based on Korteweg - de Vries equation invalid.

In 1984, Neseterenko [Nesterenko, 1983] discovered the formation and propagation of highly nonlinear solitary waves in chain of granular material. Since than, they have received a considerable attention over the last few years. Their unique character of asymmetric potential, tunability and nonlinearity has in turn led to the observation of several new phenomena of wave formation and propagation such as introduction of the concept of “sonic vacuum” due to the zero sound speed in uncompressed material.

The use of solitary waves for the detection of defects and impurities in granular media was discussed

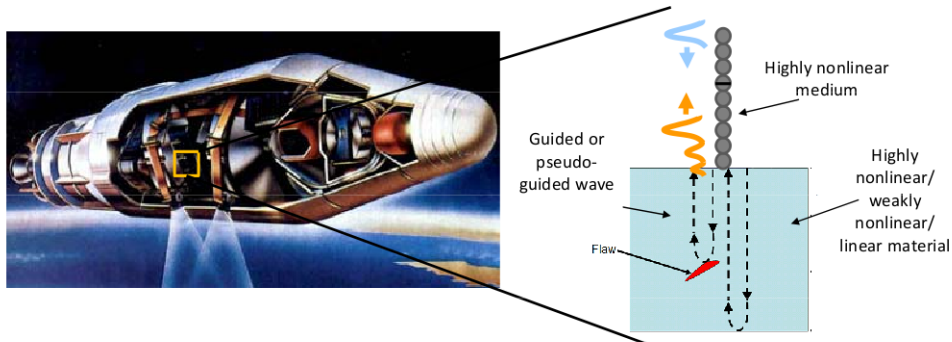


Figure 1.1: Schematic diagram of nonlinear granular chain as an automated impact actuator inside a satellite. The reflected waves from the interface, buried defect/impurity and boundaries will be used to monitor the structure.



by Sen, et al. [Sen et al., 1998] and by Hong, et.al. [Hong and Xu, 2002]. Solitary waves have been demonstrated to be sensitive to the granular materials properties [Coste et al., 1997], such as the elastic modulus, as well as to the applied static preload [Daraio et al., 2006b, Coste et al., 1997]. In addition, the dependence of the backscattered signal's velocity and shape on the presence of light and heavy impurities in a granular chain has also been noted [Hong and Xu, 2002]. C. Daraio, et al [Daraio et al., 2006a] and L. Vergara [Vergara, 2006] showed the potential usefulness of this system in energy trapping and shock disintegration work. Beside this some of the other area of application in which highly nonlinear waves can be useful are sound focusing devices (tunable acoustic lenses and delay lines), sound absorption layers, and sound scramblers [Daraio et al., 2005, Nesterenko et al., 2005, Herbold et al., 2006, Spadoni and Daraio, 2010].

## **1.2 Scope and Aim**

The goal of the project is to use the tunability and reliability of nonlinear actuator systems and to understand the coupling of nonlinear media with the adjacent linear elastic media with simple geometry and to understand the losses incorporate in the one-dimensional chain of beads, as the HNAWs travels through them.

The scope of the proposed research can be extended to the NDE/SHM to complicate engineering structures like space structures (satellites), aerospace structures (plate, stiffeners, wings, joints etc of aircrafts), ocean structures (oil rigs) and civil structures (bridges).

## **1.3 Outline of the Report**

The subsequent sections in this report are arranged as follows:

Chapter 2 reviews the background of the solitary waves in chain of granular particles. We describe our experimental setup and the conventional discrete particle model. Then it explains the finite element model developed in this project for formation and propagation of HNAWs in chain of beads.

Chapter 3 describes the dissipation losses in the nonlinear waves as they propagate in physical nonlinear actuator composed of spherical beads in one-dimensional chain.

Chapter 4 introduces the coupling of nonlinear media with adjacent linear elastic media.

Chapter 5 ends the report by discussing the main conclusions and future work possible to better understand the nonlinear actuator for NDE/SHM.

## Chapter 2

# Highly-Nonlinear acoustic waves in one-dimensional chain of spherical particles

### 2.1 Theoretical Background

Highly nonlinear acoustic waves (HNAWs) were first reported numerically, experimentally and analytically in one-dimensional granular crystals (i.e. chains of spherical particles) [Nesterenko, 2001, 1983]. Highly nonlinear media support acoustic pulses that have intrinsically different properties than those found in conventional linear acoustic signals, allowing for a stronger degree of tunability [Daraio et al., 2006b] .

Initially strongly pre-compressed, strongly nonlinear granular chains may behave as weakly nonlinear systems similar to the one considered in the Fermi-Pasta-Ulam paper [Fermi et al., 1965] . When no static pre-compression is imposed on the granules, the resulting wave equation presents no linear part: this had led to the introduction of the concept of “sonic vacuum” (SV) - a medium where no characteristic sound speed is present ( $c_0 = 0$ ) and the traditional wave equation is no longer the basic equation for representing the wave dynamics.

The general contact relation between two linear elastic particles undergoing point contact can be expressed by the nonlinear Hertzian contact law [Johnson, 1987] :

$$F = k\delta^n \quad (2.1)$$

where, ( $F$ ) is the compressive force between particle on contact with each other;  $k$  is function of the particle's material and dimension parameter (radius of contact, Poisson ratio and elastic modulus), for two identical spherical bead in contact,  $k \equiv k_s = \frac{E\sqrt{2R}}{3(1-\nu^2)}$  ;  $n$  is the nonlinear exponent (with  $n > 1$ ); and  $\delta$  is the displacement of distant point of each body. The force ( $F$ ) is considered positive in compression ( $\delta > 0$ ) and zero in tension ( $\delta < 0$ ) (particles can freely move apart from each other). The stiffness constant value  $k$  and power-law relationship  $n$  are two of the important factor in tuning the nonlinear waves, which we will explain in the following sections.

To describe the formation and propagation of the highly nonlinear solitary waves in the granular chain, Nesterenko considered particles in the chain interacting with neighboring particle according to the Hertz's Law Eq 2.1 . From this discrete system, a continuum approach based on long wavelength approximation was derived for uniform chain [Nesterenko, 1983, 2001] . The wave equation thus obtained for the highly nonlinear system is:

$$u_{tt} = -c^2 \left\{ (-u_x)^{3/2} + \frac{a^2}{10} \left[ (-u_x)^{1/4} \left( (-u_x)^{5/4} \right)_{xx} \right] \right\}_x \quad (2.2)$$

where  $u$  is the displacement,  $a$  the particle's diameter,  $c$  a material's constant, and the subscripts indicate the derivative and  $-u_x > 0$ . The constant  $c$  in Eq 2.2 is given by:

$$c^2 = \frac{2E}{\pi\rho_0(1-\nu^2)} \quad (2.3)$$

where  $E$  is the Young's modulus,  $\rho_0$  the density, and  $\nu$  the Poisson coefficient. For the case of uniform chain of granular particle, with particle interacting according to Hertzian and no or very

weak pre-compression acting on it, the exact solution for Eq 2.2 can be found as:

$$\xi = \left( \frac{5V_s^2}{4c^2} \right)^2 \cos^4 \left( \frac{\sqrt{10}}{5a}(x - V_s t) \right) \quad (2.4)$$

where  $\xi$  represents the strain and  $V_s$  the solitary wave velocity.

The solitary wave are the stress pulses that can form and travel in highly nonlinear system (i.e. granular, layered, fibrous or porous materials) with a finite spatial dimension that is independent on the wave amplitude. By a small variation of the particles assembling, for example, it is possible to significantly alter the properties (wave length, speed, amplitude, and frequency) of the excited pulse and the number of pulses in a given train [Daraio et al., 2006b]. The analytical expression for the tunability of the solitary waves speed  $V_s$  derived from the discretization of the particles in the chain can be described as follows [Daraio et al., 2006b]:

$$V_s = 0.9314 \left( \frac{4E^2 F_0}{a^2 \rho^3 (1 - \nu^2)^2} \right)^{1/6} \frac{1}{(f_r^{2/3} - 1)} \left\{ \frac{4}{15} \left[ 3 + 2f_r^{5/3} - 5f_r^{2/3} \right] \right\}^{1/2} \quad (2.5)$$

where  $F_0$  represents the static pre-stress (pre-compression) added to the system,  $f_r = F_d/F_0$  and  $F_d$  is the maximum contacts force between the particles in the discrete chain. For the case, when the system is no-pre-compressed, the Eq. 2.5 simplifies to

$$V_s = 0.6802 \left( \frac{2E}{a\rho^{3/2}(1 - \nu^2)} \right)^{1/3} F_d^{1/6} \quad (2.6)$$

In the Eq. 2.6, we see that the velocity of solitary wave  $V_s$ , is a nonlinear function of maximum dynamic force  $F_d$ , which is different than the conventional linear waves, where the wave velocity only depends on material property of the system. A plot showing the solitary wave velocity-force scaling is shown in Fig 2.3e.

Another interesting feature of the highly nonlinear solitary waves is determined by the fact that the system is size independent and the solitary waves can therefore be in principle scalable to smaller or larger dimensions, according to the needs of each specific application.

## 2.2 Experimental Setup

In our study, we analysis the a single solitary wave in the homogeneous chain of  $N$  granular particles composed of stainless steel beads (in this study  $N = 20$ , unless otherwise specified). Each bead has density ( $\rho$ ) =  $8000kg/m^3$ ; modulus of elasticity ( $E$ ) =  $193GPa$ ; Poisson's ratio ( $\nu$ ) =  $0.3$  [Carretero et al., 2009]. The beads in the experiments are supported by guided rails consisting of four rods. The rails constraint the motion of bead in one-directional.

The wave propagation within the granular chain is recorded by instrumented particles with piezo-sensors embedded in them. The piezo-sensors particles are custom fabricated in our laboratory, by introducing the piezoelectric (lead zirconate titanate) sheet ( $RC \sim 10^3\mu s$ , Piezo Systems Inc.) with custom micro-miniature wiring (supplied by Piezo Systems Inc.) between two cut halves of spherical bead (carved to accommodate wires (Fig. similar to Ref [Daraio et al., 2005])) and joining them using epoxy adhesives. The two halves of bead were fabricated such that the total mass of sensor-bead is equal to the mass of the regular beads in the chain. All sensors were connected to respective ports in Tektronix oscilloscope to monitor the force-time responses. The fabricated sensor-particles are placed at selected locations in chain to obtain the electrical signal generated during the dynamic force wave propagation in the chain. All the sensor-particles were pre-calibrated

using the momentum conservation principle. The calibration factor is used to convert the acquired data in voltage from oscilloscope to the corresponding force measured by the sensor-particle during the wave propagation [Daraio et al., 2005]

Single solitary wave is generated by impacting the chain with an identical bead as in the chain [Nesterenko, 2001]. The average wave velocity ( $V_s$ ) is measured by calculating the ratio of distance between the centers of two sensor-particle over transit time the wave takes between the two sensor-particle. The average maximum force ( $F_m$ ) between the two sensor-particle is calculated by taking the average of the force amplitude at the two sensor-particle.

## 2.3 Simulation

### 2.3.1 Discrete Particle Model

The conventional discrete particle model (DPM) for analyzing HNAWs propagation in granular chain is primarily based on the impulse-momentum law. The discrete model assumes each bead as a single point mass connected by a nonlinear spring with neighboring particle, thus imposing single degree of freedom. The nonlinear spring works according to Hertz law (Eq. 2.1) in compression and in tension it applies zero force. To compare the results obtained from DPM with experimental results, we use the nearest neighboring average method, where the force at the center of the bead is calculated by averaging the contact force on either side of the bead. This model has been used extensively to study the various properties of nonlinear waves in granular structures and was very helpful in understanding the physics of nonlinear wave propagation and interaction [Sen et al., 1998, Nesterenko et al., 2005, Vergara, 2006, Daraio et al., 2006b, Doney and Sen, 2006, Porter et al., 2008, 2009, Carretero et al., 2009].

### 2.3.2 Finite Element Model

The DPM assumes each bead as a single point mass connected by a nonlinear spring with neighboring beads. In this configuration, the bead receive an instantaneous change of motion upon impact. For a real bead, the stress generated at the contact point on one side, propagates into the interior of the bead with a finite velocity ( $c_0 = \sqrt{E/\rho}$ ) and reaches at the contact point on the other side. This phenomena of wave propagation inside the bead transfers the momentum to the next bead. During this process, the stress waves inside the bead reflects at the bounding surfaces and produces oscillations and vibrations in the bead. In order to capture the local transient deformations and stress propagation, we need modeling technique which is capable of discretizing the bead as three dimensional body instead of limiting to the single point mass assumption.

We use commercially available software Abaqus [Simulia, 2008] for modeling the granular particles as three dimensional finite element deformable bodies. Abaqus allows highly non-linear transient dynamic analysis of phenomena like impacts and multi body interaction. It also offers the possibility to manage several interactive entities simultaneously (impact of striker on bead, interaction between

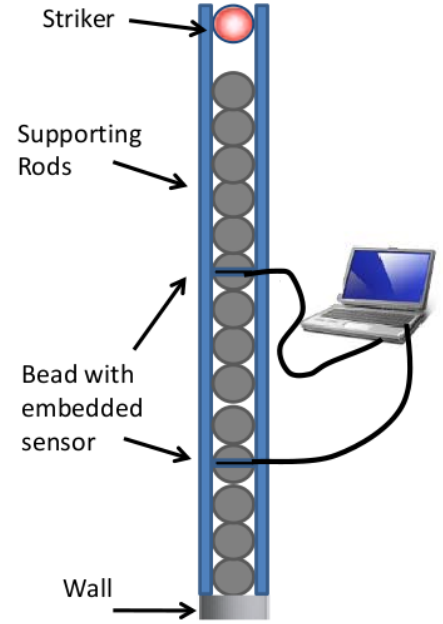


Figure 2.1: Schematic diagram of the experimental setup consisting of spherical bead particles in granular chain. Four steel rods are used as guided rail to support the beads in the chain. An identical bead is used as striker to generate single pulse of wave. Schematic shows the sensor-particle connected with computer to collect the signal data of wave propagation.

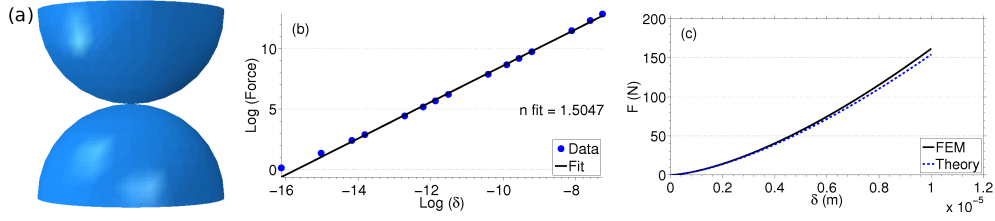


Figure 2.2: Quasi-Static Validation: (a) finite element model consisting of two spherical beads in Hertzian contact. The beads are given small displacement boundary condition and corresponding contact force is calculated from simulations. (b) the logarithmic fitting of the obtained contact force and applied displacement on the bead. The Y-axis and X-axis shows the contact force and  $\delta$  in logarithmic scale respectively. The dot values are numerically obtained contact force for the corresponding displacement, the solid line is the linear fit (c) Comparison of power law obtained from simulations (solid curve) with the Hertz's theory (Eq 2.1, dashed curve)

beads). The analysis can introduce the dynamic in a way similar to that of the experiments, managing only the impact characteristic.

In our finite element model (FEM), we use Abaqus/CAE to generate the model of the system and solve the system of equation using central-difference operator in Abaqus/Explicit. The granular beads were modeled as solid (continuum) three-dimensional elements and discretized the volume with tetrahedral elements of second order (using modified 10-node tetrahedral (C3D10M)). These elements provide a robust solution during large deformation and contact analyses and exhibit minimal volumetric and shear locking during analysis. Beads were assumed to be made of homogeneous elastic material and were modeled by using the parameters for density, Young's modulus, Poisson's ratio as presented in experimental section. For simplicity when analyzing only incoming solitary waves, we modeled the base wall as a flat rigid body composed of R3D3 type of elements.

During the wave propagation process in the chain composed of granular particles, the contact between two bodies become a crucial factor for producing a stable model. The system undergoes simultaneous multiple point contact between each neighboring particle. For this purpose, the contact interaction between two bodies was defined using the contact pair technique with surface-to-surface interaction (Explicit) in Abaqus. In this pair one of the surfaces was selected as master and the other as slave. Small-sliding kinematic constraints were applied on the contacts and zero friction in the tangential direction and contact pressure-over closure in the normal direction were used as the contact properties. The properties were selected such as to make the two bodies undergoing contact would not overlap with each other.

To validate the finite element contact model we compared it with Hertzian contact law. For this purpose we created two three-dimensional semi-spheres (Fig. 2.2a) finite element model and obtained the contact force ( $F$ ) - displacement ( $\delta$ ) relation between two beads using quasi-static assumptions. In these simulations the lower bead was held firm by applying fixed boundary conditions and the upper bead was given a displacement boundary condition. We repeated this procedure for several values of  $\delta_i$  ( $i = 1, 2, \dots, N$ ) to generate the  $F - \delta$  plot, in order to make comparison with Hertz Theory. The  $\delta_i$  values were selected such the they are insignificant compare to sphere's radius, so that small displacement assumptions of Hertz TheoryJohnson [1987]) are maintained. From the power law fitting in logarithmic scales of the contact force-displacement response obtained from the model, we get the exponent equal to  $n = 1.5047$  (Fig. 2.2b). Fig. 2.2c shows a good agreement between the  $F - \delta$  curve calculated from the finite element model using the power law obtained above with Hertz's theory (Eq 2.1).

Similarly, we perform the dynamic validation of FEM with experiments and DPM. An Abaqus model of the nonlinear granular system is shown in Fig 2.3a . Force-time plots corresponding to the waves propagation in the chain of beads are obtained for discrete particle model, finite element

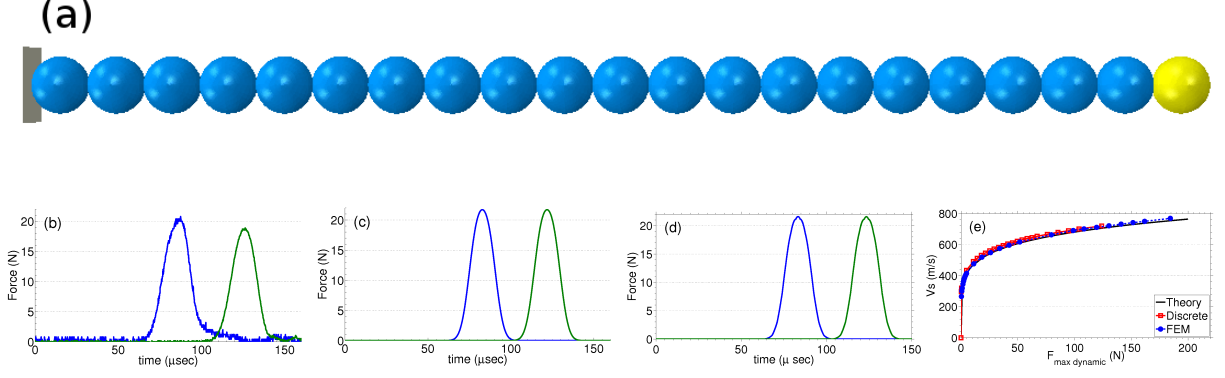


Figure 2.3: (a) Finite element model showing the one-dimensional chain of spherical beads in contact with each other Force versus time plot for the solitary wave propagation in chain composing of 20 stainless steel beads (b) Experiments, (c) Discrete Hertz Law, (d) Abaqus simulation. The curves represent the wave propagation in particle number 10 (blue) and 15 (red) respectively from the top of the chain for striker velocity  $0.626\text{m/s}$ . (e) Force-Velocity Scaling - The solid curve represents the theoretical value using Eq 2.6, the square marker represents the discrete particle model values and the dot marker represents the finite element value for Dependence of the solitary wave speed on the magnitude of the contact dynamic force.

model and in experiments assuming same initial boundary conditions and striker velocity  $0.626\text{m/s}$ . The force was measured for the 10<sup>th</sup> and 15<sup>th</sup> bead particle from the top of the chain. A comparison of the wave speed in the three different cases shows a quantitative agreement:  $641\text{m/s}$ ,  $635\text{m/s}$  and  $610\text{m/s}$  for finite element, discrete model and experiments respectively. The results obtained from finite element simulation (shown in Fig 2.3d) are in good agreement in terms of qualitative pulse shape, amplitudes and lengths with force profile calculated from discrete model (shown in Fig 2.3c) and experiments Fig 2.3b.

The relation between the solitary wave velocity  $V_s$  and maximum contact force  $F_d$  as described in Eq 2.6 for the long wave length approximation obtained from finite element is shown in Fig 2.3e along with the conventional discrete particle model and theoretical values, calculated in a similar manner as described in Ref 6. We see that the wave velocity in the finite element model goes to zero as the dynamic force decreases and agrees well with discrete particle and theoretical values. Thus the finite element model is able to describe the HNAWs in chain of beads in terms of shape, length, amplitude and velocity.

## Chapter 3

# Dissipation in one-dimensional chain of spherical particles

Dissipation plays an important role in waves propagation for physical system. The basic non-dissipative Hertzian force model is good to predict the solitary wave properties, qualitatively and quantitatively has been used extensively in most of these dynamical studies, recent experimental investigations have shown a qualitative change in force amplitude as the solitary wave propagates in the chain of spherical beads Carretero et al. [2009], Herbold et al. [2006]. These losses can be due to inherent material properties Job et al. [2005], friction between the supporting guide and beads, contact nature between neighboring particles, vibrational effects or due to uncontrolled features in the experimental setup. We developed an analytical model for DPM and also included the dissipation effects in FEM and verified them with experiments.

### 3.1 Experimental setup

We assembled a uniform monodisperse chain of  $N = 70$  particles of different materials (see Table I) with radius  $R = 2.38\text{mm}$  in a horizontal setup (as explained in section 2.2). We generated solitary waves by impacting the chain with an identical striker to the particles in the chain. The impact velocities were  $v_{imp} = [1.77, 1.55, 1.40, 1.04, 0.79](\text{m/s})$ .

### 3.2 Simulation

#### 3.2.1 Discrete Empirical Model

We model a chain of  $N$  spherical beads as a 1D lattice with Hertzian interactions [Nesterenko, 2001]:

$$\ddot{y}_n = A \left( \delta_n^{3/2} - \delta_{n+1}^{3/2} \right) + \gamma \left| \dot{\delta}_n - \dot{\delta}_{n+1} \right|^\alpha, \quad (3.1)$$

where  $s \equiv \text{sgn}(\dot{\delta}_n - \dot{\delta}_{n+1})$ ,  $A \equiv E\sqrt{2R}/[3m(1-\nu^2)]$ ,  $n \in \{1, \dots, N\}$ ,  $y_n$  is the coordinate of the center of the  $n$ -th bead,  $\delta_n \equiv \max\{y_{n-1} - y_n, 0\}$  for  $n \in \{2, \dots, N\}$ ,  $\delta_1 \equiv 0$ ,  $\delta_{N+1} \equiv \max\{y_N, 0\}$ ,  $E$  is the Young's (elastic) modulus of the beads,  $\nu$  is their Poisson ratio,  $m$  is their mass, and  $R$  is their radius. The particle  $n = 0$  represents the striker.

The  $\gamma < 0$  is the friction coefficient and  $\alpha$  is the power law for the dissipation. Both  $\alpha$  and  $\gamma$  were determined by optimizing the numerical results with experimental findings. Table 3.1 summarize our results, for three different set of experiments—using steel, teflon (polytetrafluoroethylene; PTFE),

| Material | $m$ (g) | $E$ (GPa) | $\nu$ | $\alpha$        | $\gamma$           |
|----------|---------|-----------|-------|-----------------|--------------------|
| Steel    | 0.45    | 193       | 0.30  | $1.81 \pm 0.25$ | $-5.58 \pm 1.30$   |
| PTFE     | 0.123   | 1.46      | 0.46  | $1.78 \pm 0.14$ | $-0.582 \pm 0.087$ |
| Brass    | 0.48    | 103       | 0.34  | $1.85 \pm 0.13$ | $-6.84 \pm 0.66$   |

Table 3.1: Material properties (mass  $m$ , elastic modulus  $E$ , and Poisson ratio  $\nu$ ) for stainless steel, PTFE, and brass. The last two columns present our best estimates, together with their standard deviation, of the dissipation coefficients ( $\alpha, \gamma$ ).

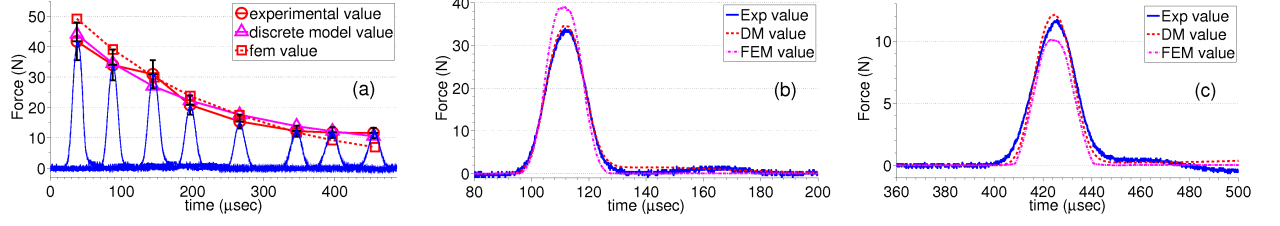


Figure 3.1: a) Decay of solitary wave in chain of 70 stainless steel particles for striker velocity =  $1.77m/s$ . The sensor-particles are placed at 9, 16, 24, 31, 40, 50, 56, and 63 bead number and the solid curves (blue) corresponds to force value observe by them. The circle with solid curve (red), the triangle with solid curve (magenta) and the square with dashed curve (red) represents the maximum value of experimental, discrete particle and finite element model respectively. b) and c)

and brass beads—in the last two columns. We found that the dissipation prefactor is material-dependent and a common exponent. This allowed us to augment the standard DPM based on Hertzian forces to encompass this dissipation effect in (optimal) quantitative agreement with our experiments.

### 3.2.2 Finite Element Model

The governing equation of motion for nonlinear dynamic response of finite element system in Abaqus is given by:

$$[M]^t \ddot{U} + [C]^t \dot{U} + [K]^t U^t = R_{ext}^t \quad (3.2)$$

The energy loss for a dissipative physical system (Eq. 3.2) is controlled by the damping matrix  $[C]^t$ . The damping matrix is modeled according to Rayleigh method, where it is assumed to be a linear combination of mass and stiffness matrices [Hughes and Cliffs, 1987].

$$C = C_M + C_K = \alpha_1 M + \alpha_2 K \quad (3.3)$$

where  $\alpha_1$  and  $\alpha_2$  are real scalars. Rayleigh parameter helps in damping lower (mass proportional) and higher (stiffness proportional) frequency signal. In our current study, because the diameter of the beads are in macroscopic range hence, the frequency of waves is on the lower side of spectrum. Therefore, the dominating factor for damping of waves in our finite element model is  $\alpha_1$  (mass proportional damping). The value of  $\alpha_1$  is determined by optimization process, which involves minimizing the residual differences ( $RMSD(\alpha_1)$ ) between numerical and experimental data.

### 3.3 Results

Fig. 3.1a shows the wave propagation obtained from the 8 sensor-particles placed in the chain, DPM Carretero et al. [2009] and FEM with dissipation included for the  $\alpha_1$  value calculated above. To better understand the effect of numerical dissipation on wave pulse, we compared the shape pulse with force profile of two sensor-particle in the experiment (one sensor-particle at the front zone and second at the rear zone of the chain respectively). Fig 3.1b and Fig 3.1c shows the force profile of experiment result for bead particle number 16 and 56 respectively, from top in solid curve (blue). The dashed curve (red) is for the discrete particle model and the dot-dashed curve (magenta) is for the finite element model with  $\alpha_1$ . We see a small local difference in the wave amplitude of finite element model for both the sensor-particle, which is evident from Fig. 3.1a, this is because the Rayleigh wave damping used in finite element model is a linear mass proportional damping. Nevertheless, the DPM and FEM is capable to captures the trend of wave amplitude decay for the over all chain (Fig 3.1a), wave pulse and velocity information within small error margin and accurately.



## Chapter 4

# Coupling of Nonlinear Media with Linear Media

One of the new applications of nonlinear acoustic wave proposed by our group is use of HNAWs for Non-Destructive Evaluation/Structural Health Monitoring (NDE/SHM) of structure [Eggenspieler et al., 2008, Daraio and Rizzo, 2008, Khatri et al., 2008, 2009]. In order to use the granular system as pulse excitation for NDE/SHM, we need to understand the wave reflection, scattering and localization at the interface of granular media and the linear media (specimen). Reflection and localization of solitary wave with rigid wall and elastic wall of various hardness has been persuaded in the past, but a complete understanding of nonlinear and linear elastic media is still lacking. In order to understand the interaction of granular media with adjacent linear media, we performed a detail study, theoretically and numerically (discrete and finite element model), of wave reflection and scattering at the interface and verify them with experiments [Yang et al., 2010] .

The experimental setup consists of 20 identical stainless steel bead particle ( $Dia = 9.525mm$ ) arranged in a vertical one-dimensional chain, with the support of rail guide. An identical bead particle is used as a striker to excite a single solitary wave in the chain. A specimen (cylindrical samples of single and double layers) is placed at the end of chain, such that the nonlinear media (granular chain) and linear elastic media (cylinder) can interact with each other. A fixed boundary condition on the far end of the cylinder is applied by clamping the base using massive V-blocks.

### 4.1 Interaction of highly nonlinear waves with a uniform medium

We studied the interaction of solitary wave with a uniform elastic media. For this study, we first varied the material of specimen keeping the geometry constant to assess the effect of mechanical properties on the reflection of the incoming solitary waves. The materials tested ranged from soft polymers to hard metals. And the second case was the study of specimen's geometry or inertia effect on the reflected signals. For this purpose, we systematically examined the stainless steel cylindrical samples of various height, keeping the radius constant. Fig. 4.1a shows the finite element model of nonlinear media interaction with single layered elastic media.

#### 4.1.1 Effects of the linear medium stiffness

As such the coupling of any two physical media has shown various interesting localized phenomenon in diverse area of physics. In our study, we found the correlation of the reflected signals on the property of adjacent linear elastic media. For the elastic modulus values below the critical limit, we found the formation of multiple (two in our case) reflected solitary pulse. The first solitary wave reflected from the interface is referred to as the primary (reflected) solitary wave (PSW), and

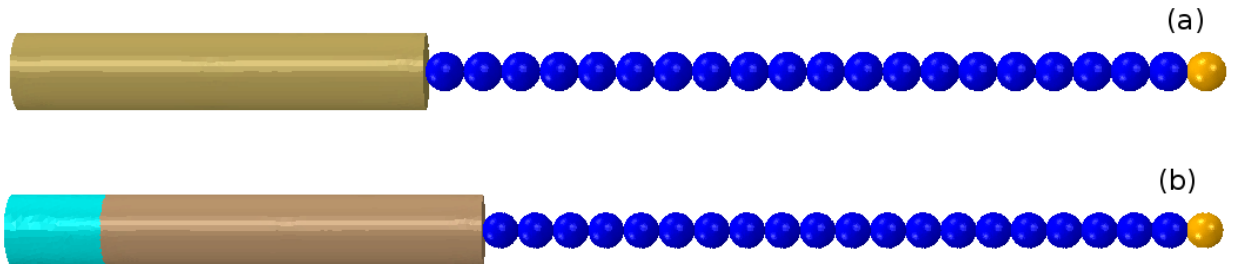


Figure 4.1: Finite element model for coupling of 1D chain of nonlinear media composed of 20 spherical beads particle with adjacent linear elastic media (a) a uniform linear medium and (b) a composite linear medium. The bottom of the linear media is under fixed boundary conditions.

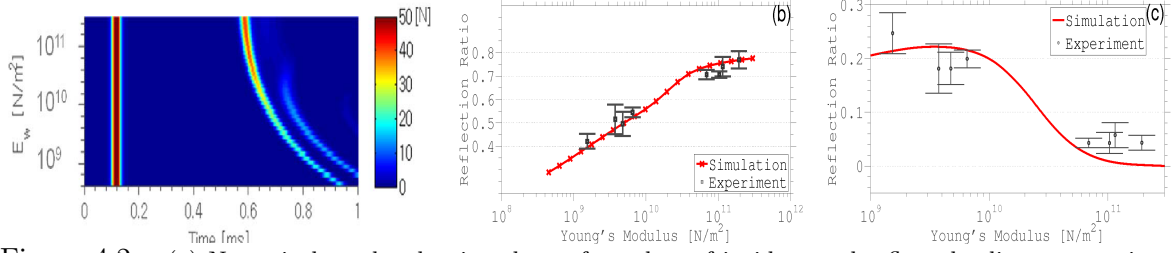


Figure 4.2: (a) Numerical results showing the surface plots of incident and reflected solitary waves in granular chain as a function of elastic modulus of the uniform linear media adjacent to the chain of spheres. The Y-axis reports a set of different values of elastic moduli of the linear media adjacent to the chain of spheres. As the stiffness of the contact is decreased, the TOF of the reflected wave increases. (b) Amplitude Reflection ratio of the amplitude of the PSW over that of the incident solitary wave. (c) Amplitude Reflection ratio of the amplitude of the SSW over the amplitude of the incident solitary wave. The reflection ratio becomes smaller as the elastic modulus increases.

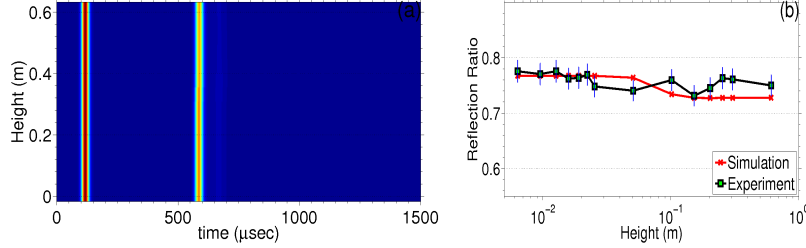


Figure 4.3: (a) Numerical results showing the surface plots of incident and reflected solitary waves in granular chain as a function of height of the uniform linear media adjacent to the chain of spheres. The Y-axis reports a set of different values of height of the linear media adjacent to the chain of spheres. The first band visible on the left represents the incoming solitary waves, while the band on the right shows the reflected solitary waves (PSWs). No secondary solitary wave is observed. (b) Amplitude Reflection ratio of the amplitude of the PSW over that of the incident solitary wave. Numerical results show a minute drop around the characteristic length of the linear medium.

the subsequent solitary wave reflected from the interface is referred to as secondary solitary wave (SSW).

For the detailed analysis, we compared the amplitude ratio (AR) and time of flight (TOF) of the primary and secondary reflected solitary wave for different values of elastic moduli of the bounding medium. Fig 4.2a shows the force intensity plot, where Y-axis is the Young's modulus and X-axis is time scale. The intensity of data represents the solitary wave amplitude. As the stiffness of the contact is decreased, the TOF of the reflected wave increases. The formation of a reflected SSW is noticeable after a critical value of elastic modulus. Adjacent media with high stiffness generates large amplitude PSW, whereas softer adjacent media produced substantially attenuate them. On the contrary to the PSW behavior, the presence of a “hard” adjacent medium produces smaller amplitude of SSWs as compared to the one generated by a “soft” adjacent medium. The plateau in the low elastic modulus range is due to the increased amount of restitutional energy losses when secondary solitary waves are generated under the interaction with a “soft” wall. The formation of SSWs disappears after a critical value of elastic modulus

#### 4.1.2 Effects of the linear medium geometry

In order to analysis the geometry effects of adjacent linear media, we used slender stainless steel cylinders of various length in wide range as specimen. In this study, we observed no SSWs despite the large variation in sample sizes tested. Also, the AR and TOF of primary reflected solitary wave is independent of the heights of the slender linear media (Fig 4.3) . The results obtained shows that the energy lost by elastic waves due to leaking into the linear media is not significant. Hence the geometry of the stainless steel cylinders has negligible effects on the wave dynamics at the linear/nonlinear interface.

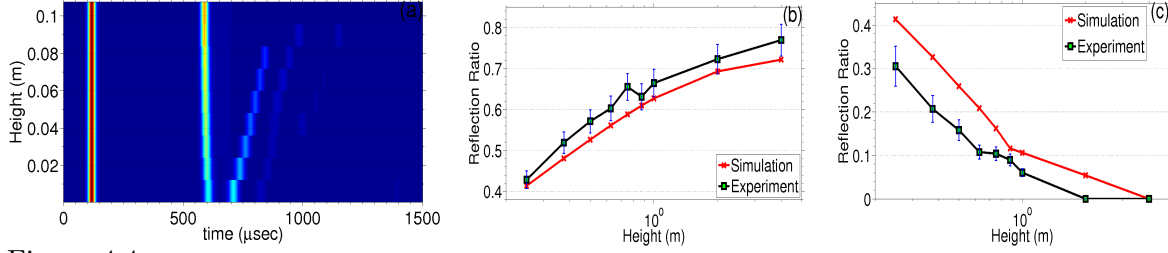


Figure 4.4: Comparison of experimental, theoretical, and numerical results for the time of arrival time on the instrumented particle (TOF) and amplitude ratio of the primary and secondary reflected solitary waves in the chain of spheres, as a function of the upper layer thickness ( $L_u$ ) in the composite media. (a) TOF for the PSWs. The arrival time is within 0.43- to 0.47-ms range. (b) Amplitude ratio for the PSWs. The amplitude reflection ratio increases as  $L_u$  grows. (c) Time of flight for the SSWs. Compared to that of the PSWs, the progression is in opposite direction with improved responsiveness. (d) Amplitude ratio of the SSWs. On the contrary to the PSW reflection in (b), larger  $L_u$  yields the smaller SSW reflection in compensation for the increased PSW reflection. For the upper layer taller than 22 mm, the magnitude of the reflection ratio drops below 10

## 4.2 Interaction of highly nonlinear waves with a composite medium

We consider the interaction of solitary waves with an adjacent composite-layered system. The nonlinear actuator system can be used in engineering applications for NDE/SHM of layers hidden underneath the surface of a composite system. The goal of this study is to understand how the nature of wave interaction and properties of reflected waves are affected by the material properties and geometry of the layered medium. Fig 4.1b shows the finite element modeled for a two layer composite medium. A stiff (stainless steel cylinder) medium is placed at the top and soft (polytetrafluoroethylene, PTFE cylinders) at the bottom. We analysis the effect of upper layer inertia on the reflected pulses by varying the height of top cylinder. We also study the influence of the lower layer cylinder on the nature of reflected waves, by varying the thickness of the bottom cylinder.

For the composite medium, the SSWs are formed because of elastic resistance of the lower medium. The initial collision of the last particle in the chain causes the translational motion in the upper layer towards the soft lower layer (PTFE layer), thereby compressing it. After the contact time, the lower medium rebound back, which results in bouncing of upper layer towards the chain. The upper medium collides with the granular chain, which triggers the formation of the SSWs.

### 4.2.1 Effects of variable thickness of the upper layer of composite medium

By varying the height of upper layer media while keeping the dimension of the PTFE base constant, we evaluate the effect of the layer mass on the solitary wave interaction. Fig 4.4a shows the intensity of wave amplitude in granular chain. The change in geometry of the upper layer affects the time of propagation of both the PSWs and SSWs as the mass of the upper layer changes (Fig 4.4b and Fig 4.4c respectively). The results shows that the arrival time and reflection ratios of the primary solitary waves are mainly governed by the mass of the upper medium. The inertia of upper media increases most of incident energy is carried by the PSWs, which result in disappearance of the secondary solitary waves.

### 4.2.2 Effects of variable thickness of the lower layer of composite medium

To understand the effects of secondary layers in composite medium on the reflected signals from nonlinear actuator, we performed study on composite medium. In this study, the upper layer mass and geometry was held constant, while varying the height of lower layer. As shown above, PSWs are generated by the initial impact of last bead with upper layer and since the upper layer is maintained same the AR and TOF of PSWs are constant for wide range of lower (PTFE) layer. The study shows that, even though the AR of SSWs is less sensitive to the height change of lower layer, the TOF of SSWs varies significantly as the thickness of the lower layer changes. The formation of

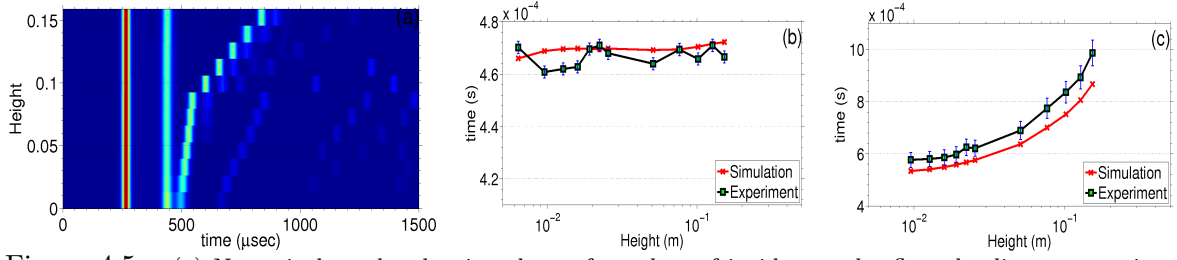


Figure 4.5: (a) Numerical results showing the surface plots of incident and reflected solitary waves in granular chain as a function of lower layer dimension of the composite linear media. The formation of the primary reflected solitary wave is insensitive to the lower layer thickness, showing the constant amplitude and arrival time for all lower layer thicknesses tested. However, the secondary solitary waves reveal significant delay in their formation as the dimension of the lower layer increases. (b) Amplitude reflection ratios of the PSWs. (c) Time of flight of the SSWs. as a function of lower medium height ( $L_d$ ).

the secondary solitary wave is delayed as the PTFE layer's thickness is increased. This is due to decrease of axial stiffness of the system as the height of lower layer is increased.

The study shows that the HNAWs interaction with the layered elastic media is affected not only by the properties of the topmost layer in contact with the nonlinear medium, but also by the properties and geometry of the lower layer. The sensitivity of the solitary waves to the change in properties of layer media will be helpful for using them in various applications like NDE/SHM.

## Chapter 5

# Conclusions and Future Work

### 5.1 Conclusions

We studied experimentally and numerically the formation and propagation of highly nonlinear solitary waves in one-dimensional homogeneous chain of granular beads, and investigated their interactions with an adjacent linear elastic medium. We have provided an empirical dissipative model to compute the propagation of highly nonlinear acoustic waves in a granular chain. This is particularly relevant, as granular chains are envisioned to function as actuators and sensors in the proposed new paradigm for NDE/SHM. We performed preliminary experimental study of coupled nonlinear and linear systems with and without structural defects, showing the advantages of using HNAWs over standard impact-echo acoustic testing systems.

In more recent studies, we observed experimentally and numerically the effects of solitary waves interacting with different single- and multi-layered media. From the analysis of waves reflected from the interface(s), we found a correlation between the properties of reflected waves and the elastic modulus of the adjacent linear elastic media. The formation of secondary solitary waves at the interface was also monitored as a function of the ratio of the elastic moduli of the linear adjacent media and of the spherical particles in the chain. For the multi-layered adjacent media, we studied the formation of secondary solitary waves as a function of the elastic properties of the second layer.

We also modeled the nonlinear granular system as a fully three-dimensional assembly using finite elements techniques in commercially available software (Abaqus). With this model we have analyzed the acoustic energy transmission at the interface between the nonlinear medium and an adjacent linear system, and monitored the reflected and transmitted acoustic wave amplitudes. The results obtained from finite element simulations were compared with experiments and a one-dimensional discrete particle model and they were found to be in good agreement in terms of qualitative and quantitative analysis.

### 5.2 Future Work

The current work for the coupling of nonlinear media and adjacent linear elastic media shows qualitative change in the wave amplitude. A better understanding and quantitative analysis of this phenomenon can be obtained by developing a theoretical model which can predict the energy distribution in surface and bulk waves in the linear elastic media. In a long term a complete detailed study will be required to use the nonlinear actuator system as an impulse excitation system for NDE/SHM of structures having defects and buried impurity. The discrete particle model will pose its limitation for modeling the nonlinear actuator system in damage detection in engineering structures. The finite element model developed in this study will be helpful in understanding some of the properties, which otherwise may be difficult to capture experimentally and hard to capture with discrete particle model.

The finite element model developed in this study can be improved to include the inelastic and viscoelastic regime of the material used for spherical beads in the chain. An introduction of plasticity and other material properties in the finite element is essential to model the engineering structure with high strain rate and impact velocity.

# Bibliography

- Ricardo Carretero, Devvrath Khatri, Mason Porter, Panayotis Kevrekidis, and Chiara Daraio. Dissipative solitary waves in periodic granular media. *Physical Review Letters*, 102(2)(024102), 2009.
- C. Coste, E. Falcon, and S. Fauve. Solitary waves in a chain of beads under hertz contact. *Physical Review E*, 56, 1997.
- Chiara Daraio and Piervincenzo Rizzo. Method and device for actuating and sensing highly nonlinear solitary waves in surfaces, structures and materials, October 2008.
- Chiara Daraio, Vitali Nesterenko, Eric Herbold, and Sungho Jin. Strongly nonlinear waves in a chain of teflon beads. *Physical Review E*, 72(016603), 2005.
- Chiara Daraio, Vitali Nesterenko, Eric Herbold, and Sungho Jin. Energy trapping and shock disintegration in a composite granular medium. *Physical Review E*, 96(058002), 2006a.
- Chiara Daraio, Vitali Nesterenko, Eric Herbold, and Sungho Jin. Tunability of solitary waves properties in one-dimensional strongly nonlinear phononic crystals. *Physical Review E*, 73(026610), 2006b.
- Robert Doney and Surajit Sen. Decorated, tapered, and highly nonlinear granular chain. *Physical Review Letters*, 97:155502, 2006.
- Damien Eggenpieler, Chiara Daraio, and Devvrath Khatri. Automated actuator device for the excitation of tunable highly nonlinear waves in granular systems, 2008.
- E Fermi, J.R Pasta, and S.M Ulam. Studies of the nonlinear problems. *University of Chicago Press*, 2(978-988), 1965.
- Eric Herbold, Vitali Nesterenko, and Chiara Daraio. Influence of controlled viscous dissipation on the propagation of strongly nonlinear waves in stainless steel based phononic crystals. APS - Shock Compression of Condensed Matter, page 1523–1526, 2006.
- Jongbae Hong and Aiguo Xu. Nondestructive identification of impurities in granular medium. *Applied Physics Letters*, 81:4868–4870, 2002.
- Thomas J. R. Hughes and Englewood Cliffs. *The Finite Element Method: Linear Static and Dynamic Finite Element Analysis*. Dover Publications, Prentice-Hall, 1987.
- Stéphane Job, Francisco Melo, Adam Sokolow, and Surajit Sen. How hertzian solitary waves interact with boundaries in a 1d granular medium. *Phys. Rev. Lett.*, 94(17):178002, May 2005. doi: 10.1103/PhysRevLett.94.178002.
- K. L. Johnson. *Contact Mechanics*. Cambridge University Press, Cambridge, 1987.
- Devvrath Khatri, Chiara Daraio, and Piervincenzo Rizzo. Highly nonlinear waves’ sensor technology for highway infrastructures. Number 6934, 69340U in Proceedings of SPIEs 15th Annual International Symposium on Smart Structures and Materials, San Diego, 2008.
- Devvrath Khatri, Chiara Daraio, and Piervincenzo Rizzo. Coupling of highly nonlinear waves with linear elastic media. Number SSN07 in SPIE Sensors and Smart Structures/NDE, 16th Annual International Symposium, San Diego, 2009.
- Vitali Nesterenko. Propagation of nonlinear compression pulses in granular media. *Journal of Appl Mech Tech*, 5(733-743), 1983.

- Vitali Nesterenko. *Dynamics of Heterogeneous Materials*. Springer-Verlag, New York, 2001.
- Vitali Nesterenko, Chiara Daraio, Eric Herbold, and Sungho Jin. Anomalous wave reflection at the interface of two strongly nonlinear granular media. *Physical Review Letters*, 95(158702), 2005.
- Mason Porter, Chiara Daraio, Eric Herbold, Ivan Szelengowicz, and Panayotis Kevrekidis. Highly nonlinear solitary waves in phononic crystal dimers. *Physical Review E*, 77(015601(R)), 2008.
- Mason Porter, Chiara Daraio, Ivan Szelengowicz, Eric Herbold, and Panayotis Kevrekidis. Highly nonlinear solitary waves in heterogeneous periodic granular media. *Physica D: Nonlinear Phenomena*, 238(666-676), 2009.
- Surajit Sen, Marian Manciu, and James D. Wright. Soliton-like pulses in perturbed and driven hertzian chains and their possible applications in detecting buried impurities. *Physical Review E*, 57:2386–2397, 1998.
- Peter Shull. *Nondestructive Evaluation: Theory, Techniques, and Applications*. Marcel Dekker, Inc, New York, 2002.
- Simulia. *Abaqus version 6.8 Documentation*. Dassault Systemes S.A., Providence, RI, 2008.
- Alessandro Spadoni and Chiara Daraio. Generation and control of sound bullets with a nonlinear acoustic lens. *Proc Natl Acad Sci USA*, 107(7230), 2010.
- Lautaro Vergara. Delayed scattering of solitary waves from interfaces in a granular container. *Physical Review E*, 73(066623), 2006.
- Jinkyu Yang, Claudio Silvestro, Devvrath Khatri, Luigi De Nardo, and Chiara Daraio. Interaction of highly nonlinear solitary waves with linear elastic media. Submitted, September 2010.